Published OnlineFirst August 11, 2009; DOI: 10.1158/1535-7163.MCT-09-0119

Sorafenib has soluble epoxide hydrolase inhibitory activity, which contributes to its effect profile *in vivo*

Jun-Yan Liu,[1] See-Hyoung Park,[3,4] Christophe Morisseau,[1,2] Sung Hee Hwang,[1] Bruce D. Hammock,[1,2] and Robert H. Weiss[2,3,4,5]

[1]Department of Entomology, [2]Cancer Research Center, [3]Comparative Pathology Graduate Group, and [4]Division of Nephrology, Department of Internal Medicine, University of California, Davis, California; and [5]U.S. Department of Veterans' Affairs Medical Center, Sacramento, California

Abstract

The advent of multikinase inhibitors targeting the vascular endothelial growth factor (VEGF) receptor has revolutionized the treatment of highly angiogenic malignancies such as renal cell carcinoma. Interestingly, several such inhibitors are commercially available, and they each possess diverse specific beneficial and adverse effect profiles. In examining the structure of sorafenib, it was hypothesized that this compound would possess inhibitory effects on the soluble epoxide hydrolase, an enzyme with pleiotropic effects on inflammation and vascular disease. We now show that sorafenib but not another VEGF receptor targeted inhibitor sunitinib is a potent inhibitor of the human soluble epoxide hydrolase *in vitro* (K_I = 17 ± 4 nmol/L). Furthermore, sorafenib causes the expected *in vivo* shift in oxylipid profile resulting from soluble epoxide hydrolase inhibition, evidence of a reduction in the acute inflammatory response. Lipopolysaccharide-induced hypotension was reversed with sorafenib but not sunitinib treatment, suggesting that soluble epoxide hydrolase inhibition accounts for at least part of the anti-inflammatory effect of sorafenib. The pharmacokinetic studies presented here in light of the known potency of sorafenib as a soluble epoxide hydrolase inhibitor indicate that the soluble epoxide hydrolase will be largely inhibited at therapeutic doses of sorafenib. Thus, it is likely that soluble epoxide hydrolase inhibition contributes to the beneficial effects from the inhibition of the VEGF receptor and other kinases during treatment with sorafenib. [Mol Cancer Ther 2009;8(8):2193–203]

Introduction

With the advent of more complete knowledge of the molecular biology of cancer, new therapies have recently been designed that target mechanisms by which the disease escapes standard therapy. For example, the multikinase and vascular endothelial growth factor (VEGF) receptor inhibitors, such as sorafenib and sunitinib (1, 2), interrupt the pathway by which angiogenesis becomes established and promulgated, resulting in inadequate nourishment of metastatic disease, thereby leading to a higher degree of treatment success. In certain malignancies such as kidney cancer, whose mechanism of oncogenesis generally involves disrupted hypoxia pathways and thus is highly angiogenic, these agents have had the effect of revolutionizing treatment.

Upon viewing the recently described X-ray crystal structure of B-Raf complexed with sorafenib (3), we noted a structural similarity between this drug (Fig. 1A) and the class of urea-based compounds (Fig. 1B) that inhibit the soluble epoxide hydrolase (4). The soluble epoxide hydrolase converts epoxyeicosatrienoic acids to the less active dihydroxyeicosatrienoic acids (5). The epoxyeicosatrienoic acids have been shown to be vasodilators in various animal models (6–10) and play an important role in regulation of blood pressure as well as control and prevention of heart disease (6, 11–14). In addition, epoxyeicosatrienoic acids are potently anti-inflammatory through mediating the nuclear factor κB and IκB kinase system (15–17). The soluble epoxide hydrolase inhibitors have been shown to stabilize the epoxyeicosatrienoic acid levels and thus have beneficial effects on hypertension (18), nociception (19), atherosclerosis (20), and inflammation (21) through increasing endogenous levels of epoxyeicosatrienoic acids and other lipid epoxides. Thus, we asked whether sorafenib possesses soluble epoxide hydrolase inhibitory activity and, consequently, whether this effect influences the known beneficial properties or adverse effects of this drug.

Although there are several VEGF receptor inhibitors commercially available (2), there exist differences in effect profiles for the various clinically available agents. Although there are minimal published studies comparing sunitinib to sorafenib in renal cell carcinoma (22), with the one available study showing a greater frequency of gastrointestinal symptoms with sunitinib (23), there is an ongoing National Cancer Institute clinical trial to attempt to address this issue

Received 2/10/09; revised 6/2/09; accepted 6/8/09; published OnlineFirst 8/11/09.

Grant support: National Institute of Environmental Health Sciences (NIEHS) grant R37 ES02710, NIEHS SBRP grant P42 ES04699, and NIH HL85727 (J-Y. Liu, C. Morisseau, and B.D. Hammock), and grant 5UO1CA86402 (Early Detection Research Network, National Cancer Institute, U.S. NIH) and grant D06CA-065 from the Morris Animal Foundation (S-H. Park and R.H. Weiss).

The costs of publication of this article were defrayed in part by the payment of page charges. This article must therefore be hereby marked *advertisement* in accordance with 18 U.S.C. Section 1734 solely to indicate this fact.

Note: Supplementary material for this article is available at Molecular Cancer Therapeutics Online (http://mct.aacrjournals.org/).

Requests for reprints: Robert H. Weiss, Division of Nephrology, Department of Internal Medicine, Genome and Biomedical Sciences Facility, University of California, Room 6312, One Shields Avenue, Davis, CA 95616. Phone: 530-752-4010; Fax: 530-752-3791. E-mail: rhweiss@ucdavis.edu

doi:10.1158/1535-7163.MCT-09-0119

Published OnlineFirst August 11, 2009; DOI: 10.1158/1535-7163.MCT-09-0119

(ClinicalTrials.gov Identifier, NCT00326898). In an attempt to explain differences in VEGF receptor inhibitor treatment outcomes as well as adverse events, we have examined the soluble epoxide hydrolase inhibitory properties of this renal cell carcinoma therapeutics.

We now show that sorafenib but not another clinically available VEGF receptor inhibitor sunitinib possesses powerful soluble epoxide hydrolase inhibitory activity. Although the soluble epoxide hydrolase inhibition showed by sorafenib shows the expected alteration in oxylipin profile in mice, such activity does not contribute to kinase inhibition or sorafenib-induced cytotoxicity shown by the VEGF inhibitors. Thus, sorafenib, in addition to its advantageous effects on tyrosine kinases, may also result in salutary effects on hypertension, inflammation, or nociception based on its property of soluble epoxide hydrolase inhibition.

Materials and Methods

Materials

The extracellular signal-regulated kinase (ERK), phospho-ERK, and β-actin antibodies were from Sigma, and the Poly (ADP-ribose) polymerase (PARP), VEGF receptor, and p-VEGF receptor were from Cell Signaling. Goat anti-mouse and goat anti-rabbit horseradish peroxidase-conjugated immunoglobulin G were obtained from Bio-Rad, and ECL Western Blotting Detection Reagents were obtained from Amersham Biosciences. Recombinant human soluble epoxide hydrolase enzymes were produced in a baculovirus expression system and purified by affinity chromatography (24, 25).

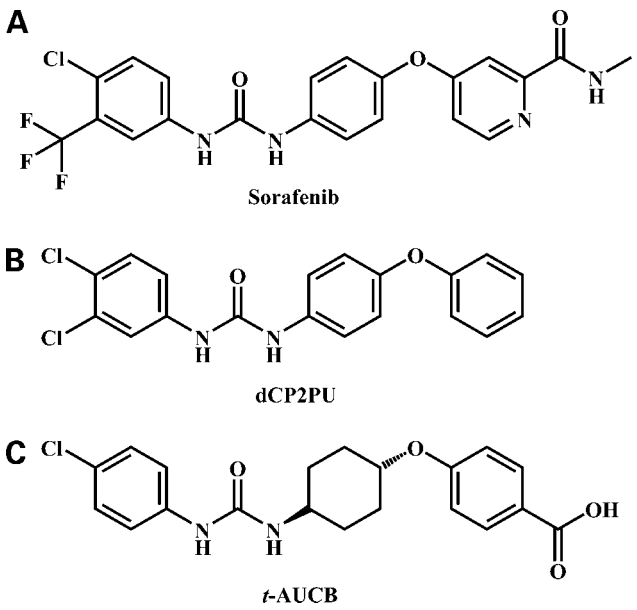

Figure 1. Structural similarity of sorafenib (**A**), dCP2PU (**B**), and *t*-AUCB (**C**; **B** and **C** are potent soluble epoxide hydrolase inhibitors; refs. 33, 54). The compound **B** (dCP2PU) is 1-(3,4-dichlorophenyl)-3-(4-phenoxyphenyl)urea and **C** (*t*-AUCB) is *trans*-4-[4-(3-adamantan-1-yl-ureido)-cyclohexyloxy]-benzoic acid, respectively.

Cell Lines

ACHN and A498 human renal cell carcinoma cells (from American Type Culture Collection) were maintained in MEM 1× media supplemented with 10% fetal bovine serum, 2 mmol/L L-glutamine, 1 mmol/L sodium pyruvate, 0.1 mmol/L nonessential amino acid, and 0.75% sodium bicarbonate at 37°C in a humidified incubator containing 5% CO_2 in air.

Measurement of Soluble Epoxide Hydrolase Inhibition

Protein concentration was quantified using the Pierce bicinchoninic acid assay with bovine serum albumin as calibrating standard. The IC_{50}s were determined by a fluorescent assay using cyano(6-methoxy-naphthalen-2-yl)methyl *trans*-[(3-phenyloxyran-2-yl)methyl] carbonate as a fluorescent substrate (26). Human soluble epoxide hydrolase was used at a concentration of 1 nmol/L that gave linear generation of product with time and protein concentration. Human soluble epoxide hydrolase was incubated with inhibitors for 5 min Bis-Tris/HCl buffer (25 mmol/L; pH 7.0) containing 0.1 mg/mL of bovine serum albumin at 30°C before substrate introduction ([S] = 5 μmol/L). Activity was measured by determining the appearance of the 6-methoxy-2-naphthaldehyde with an excitation wavelength of 330 nm and an emission wavelength of 465 nm for 10 min. Assays were done in triplicate. IC_{50} is the concentration of inhibitor that reduces enzyme activity by 50%. IC_{50} was determined by regression of at least five datum points, with a minimum of two points in the linear region of the curve on either side of the IC_{50}. Results are presented as the average ± SD of three separate measurements.

Kinetic Assay Conditions

Dissociation constants were determined following the method described by Dixon (27) for competitive tight binding inhibitors, using ^{3}H-1,3-diphenyl-*trans*-propene oxide (*t*-DPPO) as substrate (28). Inhibitor at concentrations between 0 and 50 nmol/L for sorafenib [0–25 nmol/L for 12-(3-adamantan-1-yl-ureido)-dodecanoic acid (AUDA); 0–5 nmol/L for *trans*-4-[4-(3-adamantan-1-yl-ureido)-cyclohexyloxy]-benzoic acid (*t*-AUCB); 0–200 nmol/L for 1-trifluoromethoxyphenyl-3-(1-acetylpiperidin-4-yl) urea (TPAU); 0–50 nmol/L for 1- trifluoromethoxyphenyl-3 (1-methylsulfonyl)piperidin-4-yl) urea (TUPS)] was incubated in triplicate for 5 min in sodium phosphate buffer (pH 7.4) at 30°C with 100 μL of the enzyme (1 nmol/L of human soluble epoxide hydrolase). Substrate ($3.6 < [S]_{final} < 30$ μmol/L) was then added. Velocity was measured as described (28). For each substrate concentration, the plots of the velocity as a function of the inhibitor concentration allow the determination of an apparent inhibition constant (K_{Iapp}; ref. 27). The plot of these K_{Iapp} as a function of the substrate concentration allows the determination of K_I when [S] = 0. Results are presented as average ± SE of K_I calculation.

Molecular Modeling

Molecular modeling was done using BioMedCAChe 5.0 software (Fujitsu Computer Systems Corporation). The atomic coordinates of the crystal structure of human soluble

Published OnlineFirst August 11, 2009; DOI: 10.1158/1535-7163.MCT-09-0119

Table 1. Structure and inhibition potency against the murine and human soluble epoxide hydrolases

Inhibitors Structure	Name	Inhibition of the murine sEH IC_{50} (nmol/L)	Inhibition of the human sEH IC_{50} (nmol/L)	 K_I (nmol/L)
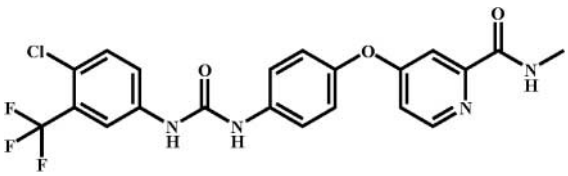	Sorafenib	30 ± 3	12 ± 2	17 ± 4
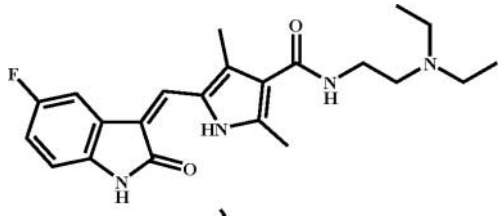	Sunitinib	17,000 ± 1,000	55,000 ± 1,000	ND
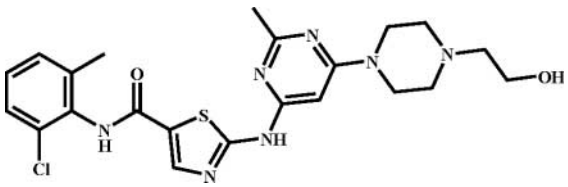	Dasatinib	27,000 ± 2,000	6,500 ± 500	ND
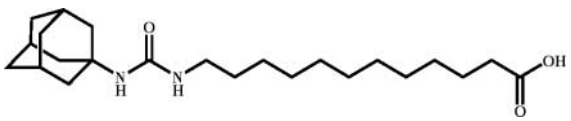	AUDA	8 ± 1	3 ± 1	6.9 ± 0.2
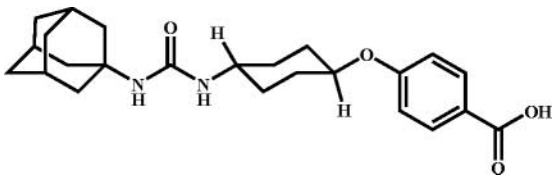	*t*-AUCB	4 ± 1	2 ± 1	1.5 ± 0.2
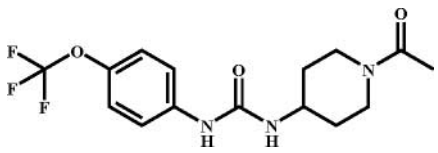	TPAU	44 ± 3	12 ± 3	57 ± 6
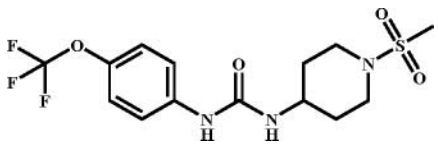	TUPS	11 ± 1	3 ± 1	14 ± 4

Abbreviations: ND, not determined; sEH, soluble epoxide hydrolase.

epoxide hydrolase complexed with the soluble epoxide hydrolase inhibitor were retrieved from Protein Data Bank (entry 1ZD3; ref. 29). The soluble epoxide hydrolase inhibitor was removed from the active site, and sorafenib was manually docked into the ligand-binding pocket by superposition with the parent molecule soluble epoxide hydrolase inhibitor. The ligand and the amino acid residues within 8.0 Å from the ligand were minimized on molecular modeling geometry.

3-(4,5-Dimethylthiazol-2-yl)-2,5-Diphenyltetrazolium Bromide (MTT) Assay

A 200 μL aliquot of cells (1×10^3 cells in quiescent media) was added to a 96-well plate and incubated for 18 h at 37°C in a humidified incubator containing 5% CO_2 in air. After incubation, the test compounds at the indicated concentration were added into each well for 48 h. Control cultures were treated with DMSO. After incubation, a 20 μL MTT solution (5 mg/mL in phosphate buffer) was added to each well, and the incubation continued for 4 h, after which time the solution in each well was carefully removed. The blue crystalline precipitate in each well was dissolved in DMSO (200 μL). The visible absorbance at 560 nm of each well was quantified using a microplate reader.

Caspase Assay

The CaspACE assay kit (Promega) was used to measure the protease activity of caspase-1 (interleukin 1β converting enzyme) and caspase-3 (32-KDa putative cysteine protease), per the manufacturer's instructions. Briefly, 2×10^6 cells per 10-cm dish were treated as described in the text. Positive control cells were treated with 4 μmol/L Camptothecin. The cells were harvested and washed, and equal protein quantities were incubated with the Asp-Glu-Vel-Asp p-nitroanilide (DEVD-pNA) caspase-3 substrate in Caspase Assay Buffer. The plates were covered with parafilm and incubated at 37°C overnight. Color development was measured at 405 nm.

Pharmacokinetics Protocol

Male Swiss-Webster mice (8 wk) were purchased from Charles River Laboratories, and experiments were done according to protocols approved by the Animal Use and Care Committee of University of California-Davis. Sorafenib tosylate (1 mg) was suspended in 1 mL trioleine and then strongly mixed on a mini vortexer for 5 min. Blood (10 μL) was collected from the tail vein using a pipette tip rinsed with 7.5% EDTA(K_3) at 0, 0.5, 1, 1.5, 2, 4, 6, 8, and 24 h after oral dosing with the inhibitor. The blood samples were prepared and analyzed according to the methods detailed in our previous study (30). Sorafenib was detected by negative model electrospray ionization tandem quadrupole mass spectrometry in multiple reaction-monitoring mode, with the precursor and dominant daughter ions of 463.0 and 193.8, respectively.

Measurement of Blood Pressure

Sorafenib and the soluble epoxide hydrolase inhibitor *t*-AUCB were dissolved in trioleine containing 10% ethanol and 10% polyethylene glycol (average molecular weight, 400; polyethylene glycol 400) to give a clear solution, whereas sunitinib gave a suspension in the same formulation solution. Male, Swiss Webster mice (8 wk) were randomly assigned to be injected i.p. with lipopolysaccharide (LPS; 10 mg/kg body weight) and immediately orally administered with sorafenib tosylate (20 mg/kg body weight, equal to 30 μmol/kg), sunitinib malate (17 mg/kg body weight, equal to 30 μmol/kg), or *t*-AUCB (1 mg/kg body weight, equal to 2.5 μmol/kg), respectively. Animals receiving oral gavage of trioleine containing 10% ethanol and 10% polyethylene glycol 400 immediately after i.p. injection of LPS or saline served as positive or negative controls, respectively. Systolic blood pressure was determined before and 24 h after treatment with noninvasive tail cuff methods using a CODA6 system (Kent Scientific Co.). For each measurement set, three acclimation cycles and 25 data cycles were used. The reported systolic blood is presented as a mean of at least five cycles of the measurement set. If the systolic blood pressure was under the detection limit, we recorded it as the detection limit (60 mmHg) for further analysis.

Metabolite Profiling Analysis of Oxylipin

Another set of animals was assigned in random to be repeatedly treated as above described. Animals were sacrificed 24 h after drug treatment. Blood was collected to separate plasma for oxylipin analysis and cytokine assay as previous reported methods (30). Plasma samples were extracted for oxylipin analysis using the methods described in (30). Plasma oxylipin were measured using an Agilent 1200 Series HPLC (Agilent Technologies, Inc.) coupled with an Applied Biosystems 4000 QTRAP hybrid, triple-quadrupole mass spectrometry instrument (Applied Biosystems). The instrument was equipped with a linear ion trap and a Turbo V ion source and was operated in negative multiple reaction-monitoring mode. Plasma oxylipins were separated using a 2.1 × 150 mm Pursuit XRs-C18 5-μm column (Varian, Inc.) held at 40°C. The gradient

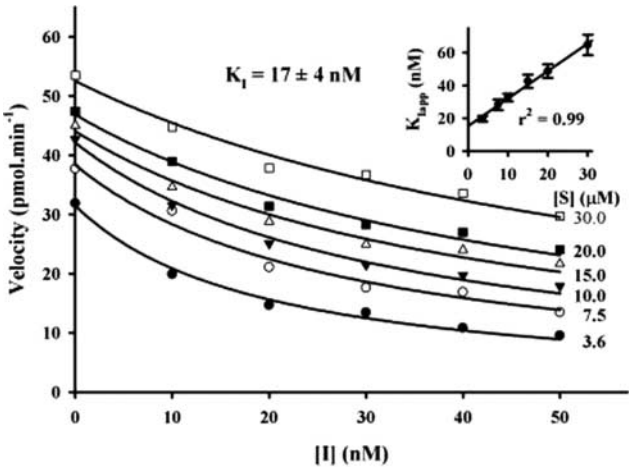

Figure 2. Determination of the K_i of sorafenib with the human soluble epoxide hydrolase (1 nmol/L) using [^{3}H]-*t*-DPPO as substrate. For each substrate concentration (3.6–30.0 μmol/L), the velocity is plotted as a function of soluble epoxide hydrolase inhibitor concentration (0–15 nmol/L), allowing the determination of an apparent inhibition constant (K_{iapp}). K_{iapp}s are plotted as a function of the substrate concentration (*inset*). For [S] = 0, a K_i value of 17 nmol/L was found. Similar plots were obtained with four other inhibitors and the human soluble epoxide hydrolase (see Table 1).

Published OnlineFirst August 11, 2009; DOI: 10.1158/1535-7163.MCT-09-0119

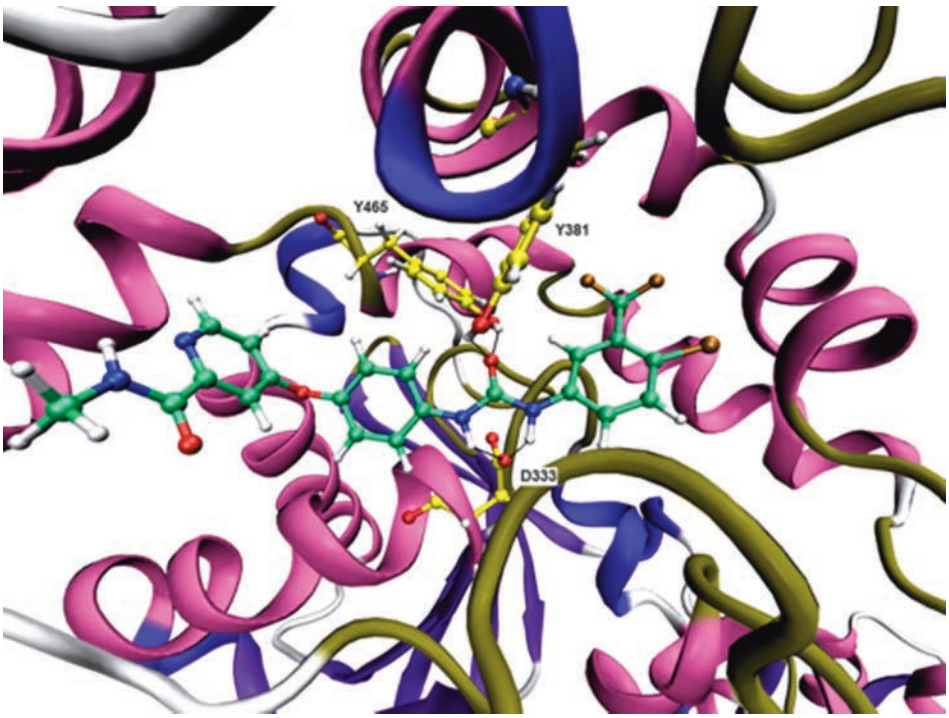

Figure 3. Docking sorafenib with the human soluble epoxide hydrolase enzyme. Sorafenib was manually docked into the active site of human soluble epoxide hydrolase. For this, we used the published X-ray crystal structure of human soluble epoxide hydrolase complex with a urea-based soluble epoxide hydrolase inhibitor (Protein Data Bank accession number 1ZD3) from http://www.rcsb.org. Between two plausible binding modes for sorafenib, the orientation given herein is the one with the lower calculated enthalpy and thus is the most probable. The opposite binding mode resulted in steric clashes with the residues of the binding site, such as Met418. Sorafenib was bound by making H-bonding interactions between the urea group and the residues Tyr381, Tyr465, and Asp333 at the active site of the human soluble epoxide hydrolase enzyme. These amino acids are shown as ball-and-stick structures on the backbone ribbon diagram.

conditions are given in Supplementary Table S1. The injection volume was 10 μL, and the samples were kept at 10°C in the autosampler. The mass spectrometers were set with a negative electrospray mode with following parameters: Curtain gas, 20 psi; Ion gas (GS) 1, 50 psi; GS2, 30 psi; Ion spray voltage, −4,500 V; Collision gas, high; temperature, 400°C; interface heater, on; and declustering potential, −60 V. The collision energies used for CAD (−18 to −38 eV) varied

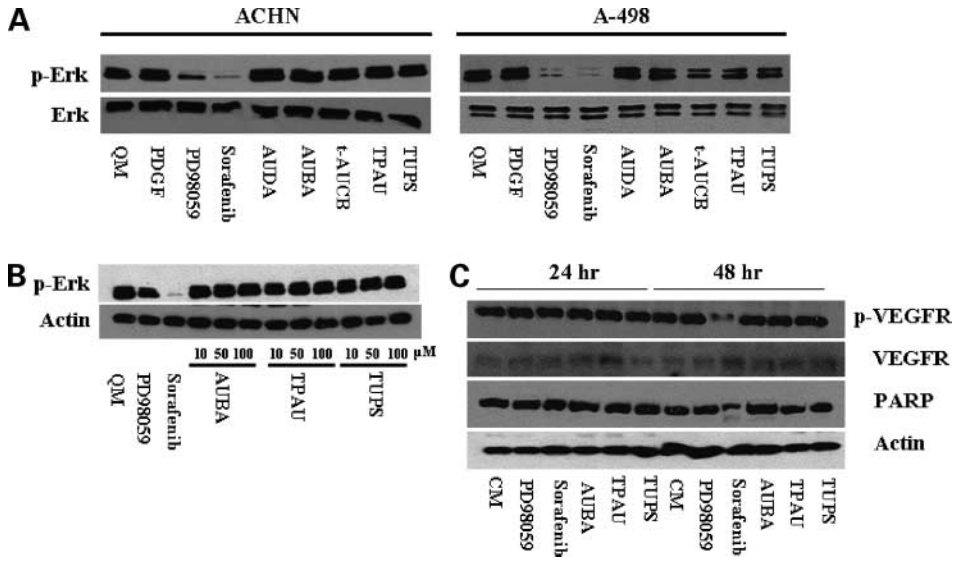

Figure 4. Conventional soluble epoxide hydrolase inhibitors of varying potency do not cause significant apoptosis or attenuate phosphorylation of ERK or VEGF receptor. **A,** ACHN and A498 cells were serum starved for 18 h and treated with vehicle (*QM lane* is serum-free quiescence media alone; vehicle is DMSO at1 μL/ml), platelet-derived growth factor, PD98059 (10 μmol/L), sorafenib (10 μmol/L), and soluble epoxide hydrolase inhibitors (10 μmol/L) for 1 h. After incubation, all cells except quiescence media control were stimulated with platelet-derived growth factor (10 ng/mL) for 15 min. Cells were harvested and immunoblotted with phospho-ERK (202Tyr204Thr) or nonphosphorylated ERK, as indicated. β-Actin is a gel loading control. **B,** ACHN cells were treated as in **A**, except that the soluble epoxide hydrolase inhibitors were treated at three different doses, as indicated. **C,** ACHN cells were treated in 10% serum-containing complete media with vehicle (DMSO at 1 μL/mL), PD98059 (10 μmol/L), sorafenib (10 μmol/L), and soluble epoxide hydrolase inhibitors (10 μmol/L) for 24 and 48 h. After incubation, cells were harvested and immunoblotted with phospho-VEGF receptor, VEGF receptor, and PARP. PARP activation is indicated by the appearance of the lower–molecular weight cleavage product. β-Actin is a gel loading control.

Published OnlineFirst August 11, 2009; DOI: 10.1158/1535-7163.MCT-09-0119

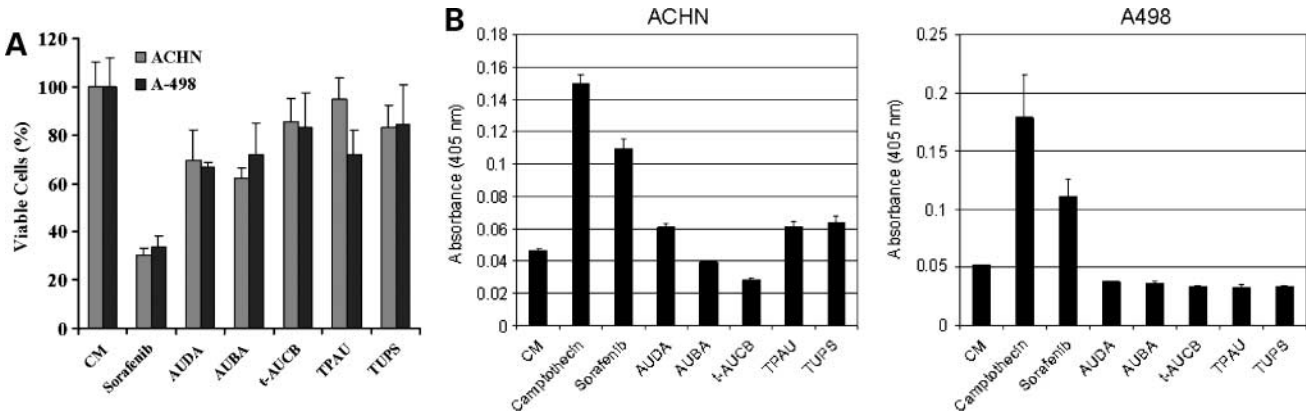

Figure 5. Conventional soluble epoxide hydrolase inhibitors of varying potency do not alter cell growth or apoptosis. ACHN and A498 cells were incubated with serum-free quiescence media for 18 h and then treated with 10% serum-containing media containing vehicle (DMSO; 1 μL/mL), sorafenib (10 μmol/L), and indicated soluble epoxide hydrolase inhibitors (10 μmol/L) for an additional 48 h. **A,** an MTT assay was done as described in Materials and Methods. The visible absorbance of each well was quantified using a microplate reader. **B,** an assay of caspase-1 and caspase-3 activity was assessed as described in Materials and Methods. The visible absorbance of each well was quantified using a microplate reader.

according to molecular species and were individually maximized for each compound. The parent and daughter ions for monitoring the target oxylipin and the corresponding parameters are presented in Supplementary Table S2. The plasma ratio of epoxyeicosatrienoic acids to dihydroxyeicosatrienoic acids was calculated for each individual animal.

Results

Sorafenib Inhibits Soluble Epoxide Hydrolase, but This Inhibitory Activity Does Not Affect Specific Kinases

Based on the structural similarity between sorafenib (3) and soluble epoxide hydrolase inhibitors (Fig. 1; ref. 29), we suspected that sorafenib might be a soluble epoxide hydrolase inhibitor. To test this hypothesis, we first measured the inhibition potency (IC_{50}) of sorafenib with the recombinant affinity purified human and murine soluble epoxide hydrolases using a fluorescent assay. As shown in Table 1, we found an IC_{50} for sorafenib of 12 nmol/L for the human and 30 for the murine soluble epoxide hydrolase enzymes, which is very similar to that of previously reported potent soluble epoxide hydrolase inhibitors, such as AUDA, *t*-AUCB, TPAU, or TUPS (31–33). Interestingly, sunitinib and dasatinib, other VEGF receptor and multikinase inhibitor, respectively (2), are not potent inhibitors of the human soluble epoxide hydrolase. To define the potency of sorafenib as a soluble epoxide hydrolase inhibitor, we determined its dissociation constant (K_I; see Fig. 2) using a radioactivity-based assay. Sorafenib has a K_I of 17 nmol/L, which is ~10-fold higher than that of the very potent *t*-AUCB but similar to the K_I of other potent soluble epoxide hydrolase inhibitors

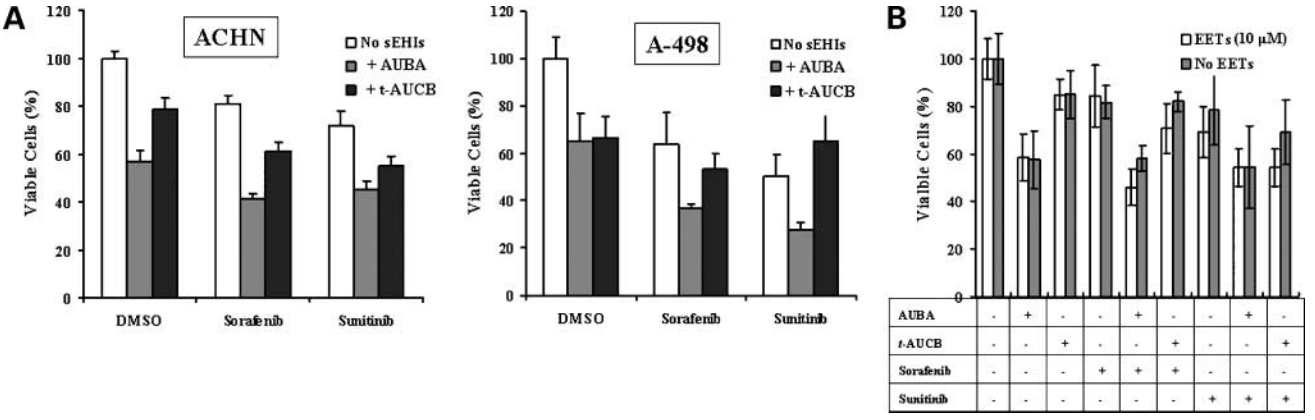

Figure 6. Neither sorafenib nor sunitinib synergizes with soluble epoxide hydrolase inhibitors on cell survival. **A,** ACHN and A498 cells were treated as described in Fig. 5 with the soluble epoxide hydrolase inhibitors AUBA and *t*-AUCB (50 μmol/L) in the presence of vehicle (DMSO), sorafenib (5 μmol/L), or sunitinib (0.5 μmol/L). **B,** ACHN cells were treated as in **A**. Epoxyeicosatrienic acids or DMSO vehicle was added to the wells at 10 μmol/L. After 48 h, the MTT assay was done as described in Materials and Methods. The visible absorbance of each well was quantified using a microplate reader.

Published OnlineFirst August 11, 2009; DOI: 10.1158/1535-7163.MCT-09-0119

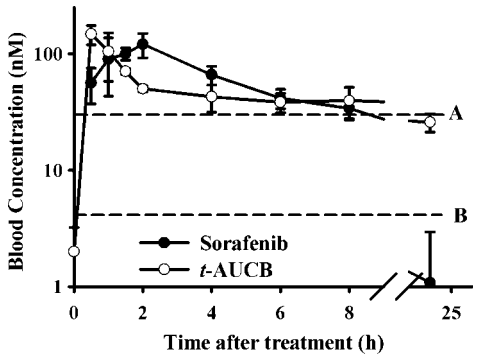

Figure 7. Blood concentration-time course of sorafenib with oral administration to mice. Sorafenib (as the tosylate at 5 mg/kg) was administered to male Swiss-Webster mice as described in Materials and Methods. Each data point is the mean ± SD of three mice plotted in a log/linear scale. Blood for sorafenib analysis was collected from the tail vein of mice at different time after oral gavage. The data of *t*-AUCB is from ref. 30. Dotted lines **A** and **B** represent the inhibitory IC_{50}s of sorafenib and *t*-AUCB against the murine soluble epoxide hydrolases, respectively.

(Table 1). Interestingly, the soluble epoxide hydrolase inhibitors TPAU and TUPS seem relatively less potent when determining K_I with a radioactive assay than determining IC_{50} with a fluorescent assay. Such discrepancy has been observed before (26).

Because sorafenib showed good inhibitory activity against soluble epoxide hydrolase, we next sought to understand how it binds to this enzyme. Sorafenib was manually docked at the active site of the human soluble epoxide hydrolase using an X-ray structure previously published (Fig. 3; ref. 29). Sorafenib was noted to be bound through H-bonding interactions with the residues Tyr381, Tyr465, and Asp333 as observed for other urea-based inhibitors (34, 35). However, unlike *t*-AUCB, sorafenib did not establish a hydrogen bond with Met418 (33). The lack of this H-bonding could explain the slightly decreased inhibitory activity of sorafenib compared with *t*-AUCB. Conversely, *t*-AUCB and other soluble epoxide hydrolase inhibitors were manually docked at the active site of the B-Raf X-ray structure (3). Interestingly, the latter compounds were able to bind by making favorable H-bonds with the urea groups in *t*-AUCB as does sorafenib, without any unfavorable interactions with other residues at the active site (data not shown), suggesting that soluble epoxide hydrolase inhibitors could inhibit B-Raf and other kinases. However, the soluble epoxide hydrolase inhibitors studied here only show the urea interaction observed between sorafenib and B-Raf (3) and not the additional favorable interactions between sorafenib and B-Raf used to explain the tight binding of sorafenib with the target kinase. Thus, there seems to be different structure-activity relationships between the soluble epoxide hydrolase inhibitors and kinase inhibitors with sorafenib being somewhat unique in being a potent inhibitor of both enzymes. The structures of many soluble epoxide hydrolase inhibitors are close enough to sorafenib that a cautious approach with inhibitor design suggests screening possible soluble epoxide hydrolase inhibitors against a library of kinases.

In addition to the soluble epoxide hydrolase inhibitory activity described above, sorafenib has well-established inhibitory activity against several kinases, including Raf, mitogen-activated protein kinase/ERK, and VEGF receptor, which by conventional wisdom accounts for its potent antiproliferative and antiangiogenic effects *in vivo* (36–38). Thus, we sought to determine whether soluble epoxide hydrolase inhibitors acted on several oncogenically relevant kinases. Although sorafenib and the MEK inhibitor PD98059 (as control) attenuate ERK phosphorylation as expected in two renal cell carcinoma cell lines, five soluble epoxide hydrolase inhibitors selected because of their varied IC_{50}s (Table 1) do not decrease ERK phosphorylation at a similar concentration (Fig. 4A and B). In addition, although sorafenib attenuates phospho-VEGF and causes apoptosis as is evidenced by PARP cleavage, there was no effect by three soluble epoxide hydrolase inhibitors with widely variable structures, K_Is, and IC_{50}s on these properties (Fig. 4C).

The Soluble Epoxide Hydrolase Inhibitors Do Not Cause Growth Inhibition or Apoptosis and Do Not Synergize with Sorafenib

Sorafenib is known to decrease cell growth and tumor vascularization and induce apoptosis; all of these are presumed mechanisms of the therapeutic effect of sorafenib in kidney cancer (39). We next asked whether the soluble epoxide hydrolase inhibitory activity of sorafenib accounts for its apoptosis or growth inhibitory effects in renal cell carcinoma cells. We used the MTT assay to assess cell growth and an assay of caspase-3 activity to measure apoptosis. Both renal cell carcinoma cell lines were incubated with sorafenib or five soluble epoxide hydrolase inhibitors for 48 hours. Although sorafenib markedly decreased cell growth (by 65–70% as compared with serum-stimulated cells), the effect of the soluble epoxide hydrolase inhibitors on cell growth was quite variable and considerably less pronounced (Fig. 5A). Furthermore, cell growth was reduced more with the weaker soluble epoxide hydrolase inhibitors, suggesting that the soluble epoxide hydrolase inhibitory activity does not correspond to renal cell carcinoma cell viability ($r^2 < 0.10$ between cell viability and inhibition potency). Sorafenib incubation also resulted in apoptosis as evidenced by activation of caspase-1 and caspase-3 activity, as expected, whereas there was no consistent such effect with the soluble epoxide hydrolase inhibitors (Fig. 5B).

If the intrinsic soluble epoxide hydrolase inhibitory activity of sorafenib contributes to its proapoptotic activity, it would be expected that soluble epoxide hydrolase inhibitors would synergize with sorafenib with respect to this property. To examine this possibility, both renal cell carcinoma cell lines were incubated with sorafenib alone, sunitinib alone (which has anti-VEGF and anti-raf activity but not soluble epoxide hydrolase inhibitory activity; see Table 1), or with one of two soluble epoxide hydrolase inhibitors having disparate IC_{50}s; these cells were subjected to an MTT assay (Fig. 6A). The experiment was repeated with the addition of exogenous epoxyeicosatrienoic acids, the substrate for soluble epoxide hydrolase (Fig. 6B). Consistent with the data described above, both soluble epoxide hydrolase

Published OnlineFirst August 11, 2009; DOI: 10.1158/1535-7163.MCT-09-0119

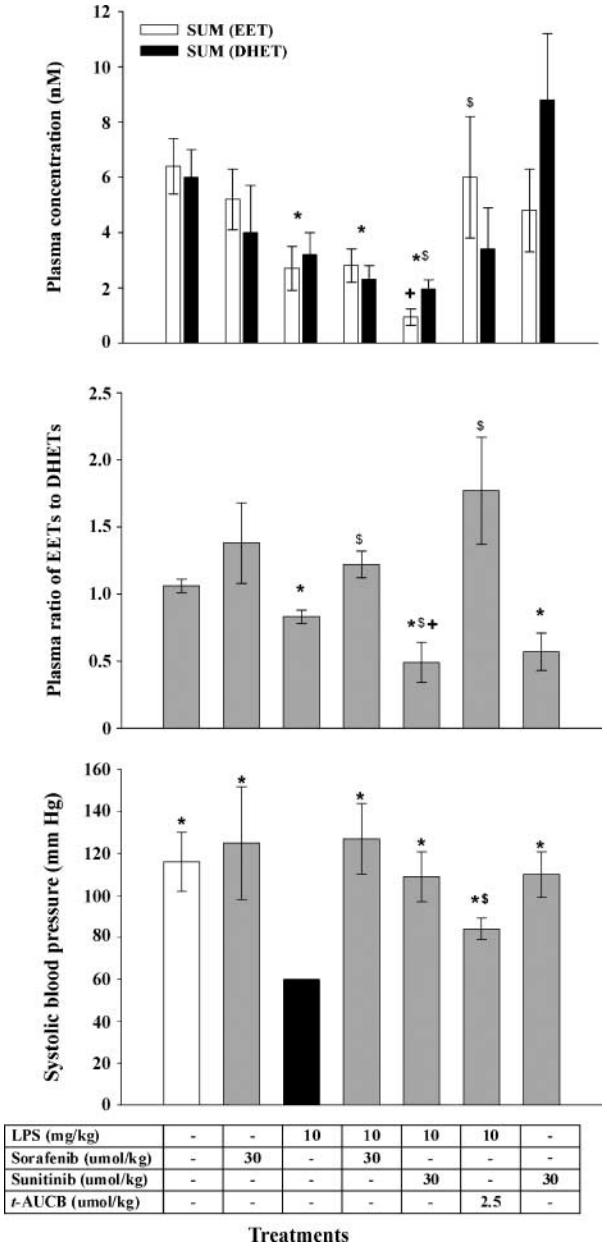

Figure 8. Sorafenib contributes to its effect profile in an LPS-challenged murine model. Animals were treated as indicated with sorafenib tosylate (30 μmol/kg), sunitinib malate salt (30 μmol/kg), or *t*-AUCB (2.5 μmol/kg), and were sacrificed 24 h after treatment. **A,** plasma level of epoxyeicosatrienoic acids (sum of 14,15-; 11,12-; and 8,9-epoxyeicosatrienoic acids; *white columns*) and dihydroxyeicosatrienoic acids (sum of 14,15-; 11,12-; and 8,9-dihydroxyeicosatrienoic acids; *black columns*). **B,** plasma ratio of total epoxyeicosatrienoic acids to total dihydroxyeicosatrienoic acids. The 5,6-epoxyeicosatrienoic acids data are excluded because of lactone formation during sample preparation. Epoxide to diol ratios in arachidonate series (20:4) are biomarkers of soluble epoxide hydrolase inhibition. **C,** systolic blood pressure was measured 24 h after treatment by a noninvasive tail cuff method. Data are mean ± SD of four individual mice for each group. *, significantly different ($P < 0.05$) from normal control; $, significantly different ($P < 0.05$) from LPS control; †, significantly different ($P < 0.05$) from the mice receiving LPS and sorafenib determined by ANOVA followed with Tukey's or Games-Howell's test.

inhibitors and both raf/VEGF inhibitors had apoptosis-inducing activity (the latter of a higher magnitude than the former), but there was no synergistic effect when the raf/VEGF inhibitors and soluble epoxide hydrolase inhibitors were added together to the cells in the presence and absence of exogenous epoxyeicosatrienoic acids. Thus, it is unlikely that the soluble epoxide hydrolase inhibitor activity inherent in sorafenib is contributing substantially to sorafenib-induced apoptosis.

Sorafenib Displays the Oxylipid Profiles of Soluble Epoxide Hydrolase Inhibition and Is Anti-inflammatory *In vivo*

Published data from our group have shown that soluble epoxide hydrolase inhibitors possess marked anti-inflammatory activity in an LPS-challenged mouse model of acute inflammation (21). To determine whether sorafenib possesses similar anti-inflammatory activity, which may be due to its soluble epoxide hydrolase inhibitor property, we first examined the pharmacokinetics of sorafenib tosylate in a murine model by oral administration at 5 mg/kg. Blood levels of sorafenib reached the maximum concentration (C_{max}) of ~120 nmol/L 2 hours after administration, and then slowly decrease such that no sorafenib could be detected after 24 hours (Fig. 7). In this system, one-compartmental analysis was shown to be the best fit model. We calculated an area under the concentration-time course curve $(AUC)_{0\text{-}24}$ of 630 nmol/L h, and an elimination half-life of 2.6 hours for sorafenib. The sorafenib pharmacokinetic profile is compared with that of *t*-AUCB used at a roughly 5× lower concentrations because of its high potency (Fig. 7). The soluble epoxide hydrolase inhibitor *t*-AUCB afforded a larger $AUC_{0\text{-}24}$ of 2,580 nmol/L h and a longer elimination half-life of >24 hours at an oral dose of 1 mg/kg (30). The compounds showed $AUC_{0\text{-}24}/IC_{50}$ (an estimate of exposure and potency) of 21 and 645 for sorafenib and *t*-AUCB, respectively. Sorafenib and *t*-AUCB had blood levels above their murine IC_{50}s for 8 and 24 hours, respectively. Compared with the results from murine model, sorafenib in man provides a higher C_{max} (>1,500 nmol/L), later T_{max} (>2 hours), longer elimination half-life (>20 hours), larger $AUC_{0\text{-}12}$ (>13,000 nmol/L h), and larger $AUC_{0\text{-}12}/IC_{50}$ (>1,080) in its phase I study even at the similar doses (40, 41).

To confirm that sorafenib inhibits soluble epoxide hydrolase *in vivo*, the epoxyeicosatrienoic acids and dihydroxyeicosatrienoic acids were measured by liquid chromatography-mass spectrometry/mass spectrometry in plasma samples taken 24 hours after treatment with LPS and then sorafenib. The termination time (24 hours) was established by a time-dependent study on sorafenib reversing the LPS-challenged hypotension. The plasma ratio of epoxyeicosatrienoic acids to dihydroxyeicosatrienoic acids characterizes the soluble epoxide hydrolase inhibition. Upon LPS challenge, the production of epoxyeicosatrienoic acids dramatically decreased as compared with nontreated animals, resulting in a significant decrease in the plasma ratio of epoxyeicosatrienoic acids to dihydroxyeicosatrienoic acids (Fig. 8A and B). Sorafenib inhibited the production of dihydroxyeicosatrienoic acids, reversing the ratio of

Published OnlineFirst August 11, 2009; DOI: 10.1158/1535-7163.MCT-09-0119

epoxyeicosatrienoic acids to dihydroxyeicosatrienoic acids to normal level. Administration of sorafenib alone inhibited the production of dihydroxyeicosatrienoic acids, resulting in a dramatic increase in the plasma ratio of epoxyeicosatrienoic acids to dihydroxyeicosatrienoic acids. As a control, administration of the soluble epoxide hydrolase inhibitor *t*-AUCB increased the production of epoxyeicosatrienoic acids, resulting in an increase in the ratio of epoxyeicosatrienoic acids to dihydroxyeicosatrienoic acids, as expected. Sunitinib, which does not possess soluble epoxide hydrolase inhibitory activity (see Table 1), inhibits the production of epoxyeicosatrienoic acids and dihydroxyeicosatrienoic acids, resulting in a decrease in the ratio of epoxyeicosatrienoic acids to dihydroxyeicosatrienoic acids. Thus, administration of sorafenib but not sunitinib to mice has the oxylipid signature of soluble epoxide hydrolase inhibition, consistent with the *in vitro* data described earlier.

As discussed above, soluble epoxide hydrolase inhibition has been shown to be anti-inflammatory in an LPS-challenged murine hypotension model (21), yet it would not be expected that kinase inhibition (as from sorafenib) would have a similar global effect (42). To determine whether sorafenib has a salutary effect on LPS-induced hypotension, we treated LPS-challenged mice with sorafenib. Although the soluble epoxide hydrolase inhibitor *t*-AUCB at 2.5 μmol/kg attenuates the hypotensive response of LPS to some degree, LPS-induced hypotension was completely reversed with sorafenib treatment (Fig. 8C), suggesting that soluble epoxide hydrolase inhibition accounts for at least part of the anti-inflammatory effect of sorafenib. Sunitinib attenuated the LPS-induced hypotensive effect to a smaller degree. However, the reduction in hypotension and the alteration in oxylipin profiles by sunitinib are much greater than that can be accounted for by its negligible soluble epoxide hydrolase inhibition, suggesting more complex mechanisms of action.

Discussion

The treatment of kidney cancer has been revolutionized by the appearance and surprising efficacy of the multikinase inhibitors sorafenib and sunitinib in heretofore chemotherapy-resistant malignancies (1). Although these drugs target many tyrosine kinases, given the high degree of angiogenesis accompanying kidney cancer, the VEGF receptor tyrosine kinase is likely the most important target of these agents in this disease. This physiology is dictated by the constitutive activation of the hypoxia-inducible factor pathway seen frequently in kidney cancer (43). However, although the VEGF receptor inhibitors possess important salutary effects on the malignancies targeted, there exist serious adverse effects associated with these treatments, most likely because of the fact that VEGF is necessary for vascular homeostasis (44). Thus, it is important to investigate other properties of the VEGF receptor inhibitors and thereby tease out mechanistic differences, which can be exploited in future refinement of this therapeutic paradigm. In this study, we have used modeling of the crystal structures to identify an unexpected property of sorafenib that begs further investigation.

Docking studies with murine and human soluble epoxide hydrolase indicated that sorafenib but not several other kinase inhibitors should be a potent inhibitor of the enzyme. Docking of several soluble epoxide hydrolase inhibitors in the B-Raf kinase catalytic site failed to show adverse interactions, cautioning that soluble epoxide hydrolase inhibitors should be screened on kinase libraries. However, the soluble epoxide hydrolase inhibitors docked failed to show the favorable interactions thought to result in the potent inhibition of sorafenib of some kinases (3). As predicted from docking studies, we showed that sorafenib but not sunitinib causes inhibition of the soluble epoxide hydrolase with the potency similar to the best available soluble epoxide hydrolase inhibitors, although these soluble epoxide hydrolase inhibitors failed to inhibit the kinases studied. This soluble epoxide hydrolase inhibition, which is likely unique among the VEGF receptor and raf inhibitors, increases the serum and/or tissue levels of epoxyeicosatrienoic acid and affects other lipid mediators that are known to have a variety of clinical effects, including the reduction of inflammation and hypertension. Although all of the ramifications of this finding have not yet been worked out, it is clear from previous work in our and other laboratories that soluble epoxide hydrolase inhibition leads to varied consequences. In the case of treatment of cancers, many of which are now considered inflammatory diseases (45, 46), soluble epoxide hydrolase inhibition may be of benefit because of its anti-inflammatory properties (21).

There also is a caution that further attenuation of inflammation by soluble epoxide hydrolase inhibition, in the presence of standard immunosuppressive compounds sometimes used in chemotherapy, may make a patient more prone to overwhelming infection. However, even complete soluble epoxide hydrolase inhibition only increases epoxyeicosatrienoic acid levels several fold. Given the available data on soluble epoxide hydrolase inhibition and blood pressure (18, 47, 48), it is possible that the soluble epoxide hydrolase inhibitory property of sorafenib may ameliorate hypertension sometimes observed with kinase inhibitor therapy. In addition, the beneficial effects of soluble epoxide hydrolase inhibition in atherosclerosis (20) may lead to beneficial end-organ protection during sorafenib therapy, and the antinociceptive effects of soluble epoxide hydrolase inhibition (19) could add to the favorable effect profile of sorafenib in cancer patients.

Our finding that sorafenib fits into the active site of soluble epoxide hydrolase (Fig. 1) based on the X-ray crystal structures previously published (3, 29) was serendipitous. Despite targeting inhibition of VEGF receptor, the other kinase inhibitors dasitinib and sunitinib do not display soluble epoxide hydrolase inhibitory activity either *in vitro* or *in vivo*, as is evidenced by their decreased levels of blood pressure and cytokine modulation as compared with that of sorafenib. Along these lines, it is indeed provocative to consider that it is the soluble epoxide hydrolase inhibitory property of sorafenib that accounts for its differences from

Published OnlineFirst August 11, 2009; DOI: 10.1158/1535-7163.MCT-09-0119

the other VEGF receptor inhibitors with respect to inflammation (42) and hypertension (49). The soluble epoxide hydrolase inhibitors are known to reduce gastrointestinal inflammation from our unpublished studies, thus the reduction in gastrointestinal and possibly cardiac side effects observed with sorafenib over sunitinib may result in part from soluble epoxide hydrolase inhibition (50). The soluble epoxide hydrolase inhibitors have been shown to dramatically reduce renal inflammation and failure for example in mice treated with the cancer drug cisplatin (51) and rats with high angiotensin levels (47). The soluble epoxide hydrolase inhibitors also are known to synergize and be synergized by low dose of indomethacin and coxibs through the cyclooxygenase pathways of the arachidonic acid cascade (19). Thus, one may be able to reduce side effects of sorafenib further with such drug combinations. However, a caution is that the stabilization of epoxyeicosatrienoic acids and other endogenous chemical mediators by soluble epoxide hydrolase inhibitors could also lead to unwanted side effects from sorafenib and other kinase inhibitors. For example the epoxyeicosatrienoic acids stabilized by soluble epoxide hydrolase inhibitors are reported to be mildly angiogenic (52, 53), and inflammation is known to be beneficial in the homeostatic response to sepsis.

Although our work shows reasons why sorafenib has a different effect profile than the other VEGF receptor inhibitors commercially available, we could find few studies directly comparing these compounds in cancer (reviewed in ref. 22), although a clinical trial to assess this is in progress. In the one available study, it was shown that both kinase inhibitors have similar side effects, although sunitinib has a higher frequency of gastrointestinal symptoms (23). However, consistent with our inflammation data, it has been shown that sorafenib but not sunitinib inhibits the secretion of cytokines and expression of CD1a from dendritic cells (42). Thus, it is possible that, in addition to our findings about tumor necrosis factor-α, there may exist more strongly differential heretofore unidentified cytokine effects with these two drugs in renal cell carcinoma that result from soluble epoxide hydrolase inhibition.

Following oral administration to mice, the soluble epoxide hydrolase inhibitor *t*-AUCB and sorafenib resulted in blood levels of active compound that are consistent with near total inhibition of the soluble epoxide hydrolase. Because the K_I of sorafenib is 10 times higher than that of *t*-AUCB, it was administered at a higher dose. As expected from their inhibitory potency sorafenib and *t*-AUCB increased the ratio of epoxyeicosatrienoic acids to dihydroxyeicosatrienoic acids to above those seen in normal control animals, even when the mice were treated with LPS. The data suggest that the very high therapeutic doses of sorafenib used for renal cancer are likely to be far excess of what is needed for inhibitor of the soluble epoxide hydrolase. A novel soluble epoxide hydrolase inhibitor is now in phase II clinical trials. The high potency of sorafenib as a soluble epoxide hydrolase inhibitor indicates that it possibly could be used for this therapeutic target at doses lower than those needed to control renal cancer.

In summary, we report a novel property of the VEGF receptor and Raf inhibitor sorafenib, which likely accounts for at least a substantial portion of its benefit and adverse effect profile. Further investigation, including *in vivo* studies, may lead to novel indications for this drug as explaining apparent benefits over other pharmaceuticals targeted kinases.

Disclosure of Potential Conflicts of Interest

No potential conflicts of interest were disclosed.

References

1. Le Tourneau C, Faivre S, Raymond E. New developments in multitargeted therapy for patients with solid tumours. Cancer Treat Rev 2008; 34:37–48.

2. Zhong HZ, Bowen JP. Molecular design and clinical development of VEGFR kinase inhibitors. Curr Top Med Chem 2007;7:1379–93.

3. Wan PTC, Garnett MJ, Roe SM, et al. Mechanism of activation of the RAF-ERK signaling pathway by oncogenic mutations of B-RAF. Cell 2004; 116:855–67.

4. Morisseau C, Goodrow MH, Dowdy D, et al. Potent urea and carbamate inhibitors of soluble epoxide hydrolases. Proc Natl Accad Sci U S A 1999; 96:8849–54.

5. Newman JW, Morisseau C, Hammock BD. Epoxide hydrolases: their roles and interactions with lipid metabolism. Prog Lipid Res 2005;44: 1–51.

6. Seubert JM, Zeldin DC, Nithipatikom K, Gross GJ. Role of epoxyeicosatrienoic acids in protecting the myocardium following ischemia/reperfusion injury. Prostag Oth Lipid M 2007;82:50–9.

7. Imig JD, Falck JR, Navar LG. 11,12-Epoxyeicosatrienoic acid (11,12-Eet) is a potent vasodilator of the renal microvasculature. J Am Soc Nephrol 1995;6:679.

8. Carroll MA, Schwartzman ML, Capdevila J, et al. Vascular activity of 5,6 epoxyeicosatrienoic acid. Clin Res 1987;35:A266–A.

9. Carroll MA, Schwartzman M, Capdevila J, Falck JR, McGiff JC. Vasoactivity of arachidonic acid epoxides. Eur J Pharmacol 1987;138:281–3.

10. Pomposiello SI, Quilley J, Carroll MA, Falck JR, McGiff JC. 5,6-Epoxyeicosatrienoic acid mediates the enhanced renal vasodilation to arachidonic acid in the SHR. Hypertension 2003;42:548–54.

11. Imig JD. Epoxide hydrolase and epoxygenase metabolites as therapeutic targets for renal diseases. Am J Physiol-Renal 2005;289: F496–503.

12. Sarkis A, Roman RJ. Role of *cytochrome P*450 metabolites of arachidonic acid in hypertension. Curr Drug Metab 2004;5:245–56.

13. Elbekai RH, El-Kadi AOS. *Cytochrome P*450 enzymes: central players in cardiovascular health and disease. Pharmacol Therapeut 2006;112: 564–87.

14. Doggrell SA. *Cytochrome P*-450: a new target in the heart and coronary circulation. Drug Future 2005;30:261–9.

15. Campbell WB. New role for epoxyeicosatrienoic acids as anti-inflammatory mediators. Trends Pharmacol Sci 2000;21:125–7.

16. Xu D, Li N, He Y, et al. Prevention and reversal of cardiac hypertrophy by soluble epoxide hydrolase inhibitors. Proc Natl Accad Sci U S A 2006; 103:18733–8.

17. Node K, Huo YQ, RuiningXL , et al. Anti-inflammatory properties of *cytochrome P*450 epoxygenase-derived eicosanoids. Science 1999;285: 1276–9.

18. Jung O, Brandes RP, Kim IH, et al. Soluble epoxide hydrolase is a main effector of angiotensin II-induced hypertension. Hypertension 2005;45: 759–65.

19. Schmelzer KR, Inceoglu B, Kubala L, et al. Enhancement of antinociception by coadministration of nonsteroidal anti-inflammatory drugs and soluble epoxide hydrolase inhibitors. Proc Natl Acad Sci U S A 2006; 103:13646–51.

20. Ulu A, Davis BB, Tsai HJ, et al. Soluble epoxide hydrolase inhibitors reduce the development of atherosclerosis in apolipoprotein E-knockout mouse model. J Cardiovasc Pharmacol 2008;52:314–23.

21. Schmelzer KR, Kubala L, Newman JW, et al. Soluble epoxide hydrolase

is a therapeutic target for acute inflammation. Proc Natl Acad Sci U S A 2005;102:9772–7.

22. Hiles JJ, Kolesar JM. Role of sunitinib and sorafenib in the treatment of metastatic renal cell carcinoma. Am J Health-Syst Ph 2008; 65:123–31.

23. Herrmann E, Bierer S, Gerss J, et al. Prospective comparison of sorafenib and sunitinib for second-line treatment of cytokine-refractory kidney cancer patients. Oncol Basel 2008;74:216–22.

24. Wixtrom RN, Silva MH, Hammock BD. Affinity purification of cytosolic epoxide hydrolase using derivatized epoxy-activated sepharose gels. Anal Biochem 1988;169:71–80.

25. Beetham JK, Tian TG, Hammock BD. cDNA cloning and expression of a soluble epoxide hydrolase from human liver. Arch Biochem Biophys 1993;305:197–201.

26. Jones PD, Wolf NM, Morisseau C, et al. Fluorescent substrates for soluble epoxide hydrolase and application to inhibition studies. Anal Biochem 2005;343:66–75.

27. Dixon M. Graphical determination of *K*m and *K*i. Biochem J 1972;129: 197–&.

28. Borhan B, Mebrahtu T, Nazarian S, Kurth MJ, Hammock BD. Improved radiolabeled substrates for soluble epoxide hydrolase. Anal Biochem 1995;231:188–200.

29. Gomez GA, Morisseau C, Hammock BD, Christianson DW. Human soluble epoxide hydrolase: structural basis of inhibition by 4-(3-cyclohexylureido)-carboxylic acids. Protein Sci 2006;15:58–64.

30. Liu JY, Tsai HJ, Hwang SH, et al. Pharmacokinetic optimization of four soluble epoxide hydrolase (sEH) inhibitors for use in a murine model of inflammation. Br J Pharmacol 2009;156:284–96.

31. Morisseau C, Goodrow MH, Newman JW, et al. Structural refinement of inhibitors of urea-based soluble epoxide hydrolases. Biochem Pharmacol 2002;63:1599–608.

32. Jones PD, Tsai HJ, Do ZN, Morisseau C, Hammock BD. Synthesis and SAR of conformationally restricted inhibitors of soluble epoxide hydrolase. Bioorg Med Chem Lett 2006;16:5212–6.

33. Hwang SH, Tsai HJ, Liu JY, Morisseau C, Hammock B. Orally bioavailable potent soluble epoxide hydrolase (sEH) inhibitors. J Med Chem 2007; 50:3825–40.

34. Argiriadi MA, Morisseau C, Goodrow MH, et al. Binding of alkylurea inhibitors to epoxide hydrolase implicates active site tyrosines in substrate activation. J Biol Chem 2000;275:15265–70.

35. Gomez GA, Morisseau C, Hammock BD, Christianson DW. Structure of human epoxide hydrolase reveals mechanistic inferences on bifunctional catalysis in epoxide and phosphate ester hydrolysis. Biochemistry-Us 2004;43:4716–23.

36. Al Hazzouri A, Vaziri SA, Lynch M, et al. Anti-proliferative effects of sorafenib in clear cell renal cell carcinoma (CCRCC) cell lines: relationship to von Hippel Lindau protein (pVHL) expression and hypoxia. J Clin Oncol 2006;24:241s–s.

37. Reganti S, Kabba E, Stock W, et al. Anti-angiogenic effects of sorafenib in relapsed chronic lymphocytic leukemia: correlative studies of a phase 2 clinical trial. Blood 2007;110:255b–b.

38. Silay MS, Miroglu C. Sunitinib malate and sorafenib may be beneficial at the treatment of advanced bladder cancer due to their anti-angiogenic effects. Med Hypotheses 2007;69:892–5.

39. Chang YS, Adnane J, Trail PA, et al. Sorafenib (BAY 43-9006) inhibits tumor growth and vascularization and induces tumor apoptosis and hypoxia in RCC xenograft models. Cancer Chemoth Pharm 2007;59:561–74.

40. Minami H, Kawada K, Ebi H, et al. Phase I and pharmacokinetic study of sorafenib, an oral multikinase inhibitor, in Japanese patients with advanced refractory solid tumors. Cancer Sci 2008;99:1492–8.

41. Strumberg D, Clark JW, Awada A, et al. Safety, pharmacokinetics, and preliminary antitumor activity of sorafenib: a review of four phase I trials in patients with advanced refractory solid tumors. Oncologist 2007;12:426–37.

42. Hipp MM, Hilf N, Walter S, et al. Sorafenib, but not sunitinib, affects function of dendritic cells and induction of primary immune responses. Blood 2008;111:5610–20.

43. Weiss RH, Lin PY. Kidney cancer: identification of novel targets for therapy. Kidney Int 2006;69:224–32.

44. Lee S, Chen TT, Barber CL, et al. Autocrine VEGF signaling is required for vascular homeostasis. Cell 2007;130:691–703.

45. Pollard JW. Tumour-educated macrophages promote tumour progression and metastasis. Nat Rev Cancer 2004;4:71–8.

46. Balkwill F, Mantovani A. Inflammation and cancer: back to Virchow? Lancet 2001;357:539–45.

47. Imig JD, Zhao XY, Zaharis CZ, et al. An orally active epoxide hydrolase inhibitor lowers blood pressure and provides renal protection in salt-sensitive hypertension. Hypertension 2005;46:975–81.

48. Imig JD, Zhao XY, Capdevila JH, Morisseau C, Hammock BD. Soluble epoxide hydrolase inhibition lowers arterial blood pressure in angiotensin II hypertension. Hypertension 2002;39:690–4.

49. Obhrai JS, Patel TV, Humphreys BD. The case—progressive hypertension and proteinuria on anti-angiogenic therapy. Kidney Int 2008;74: 685–6.

50. Bhojani N, Jeldres C, Patard JJ, et al. Toxicities associated with the administration of sorafenib, sunitinib, and temsirolimus and their management in patients with metastatic renal cell carcinoma. Eur Urol 2008;53: 917–30.

51. Parrish AR, Chen G, Burghardt RC, et al. Attenuation of cisplatin nephrotoxicity by inhibition of soluble epoxide hydrolase. Cell Biol Toxicol 2009;25:217–25.

52. Wang Y, Wei X, Xiao X, et al. Arachidonic acid epoxygenase metabolites stimulate endothelial cell growth and angiogenesis via mitogen-activated protein kinase and phosphatidylinositol 3-kinase/Akt signaling pathways. J Pharmacol Exp Ther 2005;314:522–32.

53. Pozzi A, Macias-Perez I, Abair T, et al. Characterization of 5,6- and 8,9-epoxyeicosatrienoic acids (5,6- and 8,9-EET) as potent in vivo angiogenic lipids. J Biol Chem 2005;280:27138–46.

54. McElroy NR, Jurs PC, Morisseau C, Hammock BD. QSAR and classification of murine and human soluble epoxide hydrolase inhibition by urea-like compounds. J Med Chem 2003;46:1066–80.

AACR American Association for Cancer Research

Molecular Cancer Therapeutics

Sorafenib has soluble epoxide hydrolase inhibitory activity, which contributes to its effect profile *in vivo*

Jun-Yan Liu, See-Hyoung Park, Christophe Morisseau, et al.

Mol Cancer Ther 2009;8:2193-2203. Published OnlineFirst August 11, 2009.